

# Vascular healing and integration of a fully bioresorbable everolimus-eluting scaffold in a rabbit iliac arterial model

Marc Vorpahl<sup>1</sup>, MD; Masataka Nakano<sup>1</sup>, MD; Laura E. L. Perkins<sup>2</sup>, DVM, PhD; Fumiyuki Otsuka<sup>1</sup>, MD, PhD; Russell Jones<sup>1</sup>; Eduardo Acampado<sup>1</sup>, DVM; Jennifer P. Lane<sup>2</sup>, BS; Richard Rapoza<sup>2</sup>, PhD; Frank D. Kolodgie<sup>1</sup>, PhD; Renu Virmani<sup>1\*</sup>, MD

1. CVPath Institute Inc., Gaithersburg, MD, USA; 2. Abbott Vascular, Santa Clara, CA, USA

## KEYWORDS

- bioresorbable scaffold
- everolimus
- histology
- rabbit
- stent

## Abstract

**Aims:** We aimed to investigate a fully bioresorbable poly-L-lactide (PLLA) scaffold to assess vascular remodeling in comparison to a permanent polymeric metal DES.

**Methods and results:** Twenty-five New Zealand white rabbits received an Absorb bioresorbable vascular scaffold (BVS, 1.0 and 1.1) or a CYPHER<sup>®</sup> sirolimus-eluting stent (SES) in the iliac arteries. Twelve arteries were harvested at one month for scanning electron microscopy (SEM) analysis (BVS 1.1). The other implanted (BVS 1.0) arteries (n=32) were explanted at three, six and 36 months for light microscopic analysis. Re-endothelialisation assessed at one month was incomplete in both BVS and SES by SEM, with a trend towards greater coverage in SES (endothelialisation above strut: 32.2% vs. 60.6%, p=0.10). However, light microscopic analysis at later time points revealed greater endothelial coverage in BVS than in SES at 36 months (100.0% vs. 93.3%, p=0.05). Inflammation scores were comparable between arteries implanted with BVS and SES at three months (1.1 vs. 1.1, p=0.99), which decreased over time in the BVS implanted arteries (36 months: 0.0 vs. 0.2, p=0.05). At 36 months, BVS were completely resorbed, and resorption sites were replaced by connective tissue.

**Conclusions:** BVS in the rabbit iliac artery model demonstrated ongoing vascular healing at three and six months, and complete vessel restoration, re-endothelialisation and no to minimal vascular inflammation at 36 months.

\*Corresponding author: CVPath Institute, Inc., 19 Firstfield Rd, Gaithersburg, MD, 20878, USA.

E-mail: rvirmani@cvpath.org

## Abbreviations

- BVS** bioresorbable vascular scaffold  
**DES** drug-eluting stent  
**SES** sirolimus-eluting stent

## Introduction

While drug-eluting stents (DES) have resulted in remarkable benefits by lowering the incidence of restenosis as compared to bare metal stents, new concerns have arisen regarding the safety of these devices, since clinical studies have shown an increased risk of late stent thrombosis (LST) in patients receiving DES<sup>1</sup>. Histologic studies have shown delayed vessel healing as the primary mechanism of this severe adverse event where poor re-endothelialisation is the best known surrogate linked to the occurrence of LST in man<sup>2,3</sup>.

The drug release in first- and second-generation DES technologies is controlled by permanent polymers. For first-generation DES, the long-term presence of these polymers has been suggested to be associated with hypersensitivity reactions and/or strut malapposition secondary to excessive fibrin deposition<sup>4,5</sup>. In addition, metallic stents are associated with impaired restoration of vasomotion with endothelial dysfunction, which may contribute to the development of neoatherosclerosis that leads to late adverse events such as in-stent restenosis and LST<sup>6</sup>. However, reintervention may then be precluded by the “full metal jacket” imparted by implanted stents. Therefore, the concept of a fully bioresorbable scaffold which avoids these detractions of permanent metallic implants is attractive. The Absorb everolimus-eluting bioresorbable vascular scaffold (BVS) (Abbott Vascular, Santa Clara, CA, USA), which consists of a fully resorbable backbone of poly-L-lactide (PLLA) coated with poly-D, L-lactide (PDLLA) that elutes everolimus, has shown promising long-term results both in a preclinical porcine animal model<sup>7</sup> and in the ABSORB clinical trials<sup>8-14</sup>.

To further advance our understanding of the biological responses to a bioresorbable scaffold and permanent polymeric stents in the rabbit iliac artery model, we investigated BVS in a non-atherosclerotic rabbit iliac artery model at one, three, six and 36 months.

## Methods

### RABBIT MODEL OF DEVICE IMPLANTATION

The study protocol was reviewed and approved by the Institutional Animal Care and Research Committee, MedStar Research Institute Animal Facility (MRI) at Washington Hospital Center (Washington, DC). Under general anaesthesia, adult male New Zealand White rabbits (3.7-4.1 kg) underwent endothelial denudation of both iliac arteries using a balloon catheter. Subsequently, an Absorb everolimus-eluting bioresorbable vascular scaffold (BVS) (3.0×12 mm, BVS 1.1 for SEM analysis, BVS 1.0 for light microscopic analysis), or a CYPHER<sup>®</sup> sirolimus-eluting stent (SES) (Cordis Corp., Johnson & Johnson, Warren, NJ, USA) (3.0×13 mm) was deployed in the iliac arteries at the site of injury at nominal pressure to achieve a target device-to-artery ratio of 1.3:1. The duration of BVS implantation was at least 30 sec with gradual pressure increase by 2 atm every five sec up to the nominal pressure. The BVS 1.0 and 1.1 are analogous to

devices used in the ABSORB cohort A and B clinical trials, respectively<sup>9,13</sup>, with the BVS 1.0 device being the same as that evaluated in a porcine model<sup>7</sup>. The second-generation BVS (BVS 1.1) has similar composition and strut thickness to the first-generation BVS (BVS 1.0), but has a better scaffold design and improved manufacturing process which provides a more uniform and greater vessel wall support with a lower hydrolysis rate (*in vivo* degradation) of the polymer<sup>12</sup>. Because the BVS (1.0) used in these light microscopy studies share the same material compositions, vascular responses observed at the selected time points in this preclinical model are expected to translate to the current iteration of the device.

Rabbits were anticoagulated with aspirin, 40 mg/day, orally (approximately 10 mg/kg) 24 hours before catheterisation with continued dosing throughout the in-life phase of the study. Single-dose intra-arterial heparin (150 IU/kg) was administered at the time of catheterisation. Following device implantation, post-procedural angiography was performed to document vessel patency, and the animals were allowed to recover.

### HARVEST OF IMPLANTED ARTERIES

The implanted arteries were harvested at one, three, six and 36 months after implantation. All implanted arteries were fixed *in situ* with 10% neutral buffered formalin after perfusion with Ringer's lactate to remove blood. Implanted arteries for scanning electron microscopy (SEM) were cut longitudinally, photographed and processed as previously described<sup>15</sup>. For light microscopy (three, six and 36 months), the implanted arteries were dehydrated in a graded series of ethanol and embedded in methyl methacrylate plastic. After polymerisation, two to three millimetre sections were sawn from the proximal, middle, and distal treated portions of each implanted artery. Sections were cut on a rotary microtome at 6 µm, mounted on charged glass slides, and stained with haematoxylin and eosin, and Movat pentachrome.

### SEM ANALYSIS

Composites of serial *en face* SEM images were acquired at ×15 magnification and assembled to provide a complete view of the entire luminal surface of the implanted arteries. The images were further enlarged (×200 magnification), allowing direct visualisation of endothelial cells. The extent of luminal endothelial surface coverage above and between struts was evaluated from the acquired images, and the results were expressed as the percentage of total surface area above or between struts for endothelial coverage<sup>15,16</sup>.

### MORPHOMETRY AND HISTOLOGY

All arterial segments were examined blinded to treatment. Vessel injury score was calculated according to the Schwartz method<sup>17</sup>. Computerised planimetry was performed on all implanted arterial sections. The cross-sectional areas (external elastic lamina [EEL], internal elastic lamina [IEL], and lumen) of each section were measured with digital morphometry. Area measurements were used to calculate the following parameters: medial area=EEL-IEL area, neointimal area=IEL-lumen area, % stenosis=(1-[lumen area/IEL area]×100).

Neointimal thickness was measured as the distance from the IEL to the luminal border in the areas between struts/resorption sites for both SES and BVS. The presence of fibrin deposition and giant cell infiltration around the struts/resorption sites was assessed and expressed as a percentage of the total number of struts/resorption sites in each section. Neointimal inflammation and fibrin were evaluated and scored (value 0-3) as previously reported<sup>18</sup>. Endothelial coverage was visually estimated and expressed as the percentage of the lumen circumference covered by endothelium. Additional stains were performed for the identification of proteoglycans (Alcian blue), smooth muscle cells (HHF-35), and endothelium (factor VIII)<sup>7,19</sup>.

### STATISTICAL ANALYSIS

Values were expressed as mean±SD. Normality of distribution was tested with the Shapiro-Wilk test. Statistical comparison for normally distributed data was performed using the Student's t-test. For the comparison of non-normally distributed data, the Wilcoxon rank-sum test was used. A p-value of ≤0.05 was considered statistically significant.

## Results

### ANIMAL CONDITION AND OUTCOMES

A total of 44 devices (SEM, one month: six BVS [BVS 1.1] and six SES; light microscopy, three months: eight BVS [BVS 1.0] and eight SES; six months: three BVS [BVS 1.0] and three SES; 36 months: five BVS [BVS 1.0] and five SES) were successfully implanted in 25 rabbits without any complications. All animals survived the in-life phase of the study and were included in the final analysis.

### SEM ANALYSIS OF ENDOTHELIALISATION AT ONE MONTH

Scanning electron microscopy of BVS 1.1 implanted arteries at one month demonstrated incomplete endothelial coverage with mild

platelet and fibrin deposition as well as inflammatory cell infiltration, particularly over the exposed struts (**Figure 1**). The endothelial coverage of the BVS was observed especially at the proximal and distal regions, with only limited coverage of struts in the middle region of the scaffold. Overall, BVS showed a trend towards lesser endothelialisation than SES above struts (32.2±22.8% vs. 60.6±30.0%, p=0.10) and similar coverage between struts (87.8±4.6% vs. 90.6±4.9%, p=0.33). However, endothelial coverage above struts was variable among scaffolds as demonstrated by a relatively large standard deviation.

### HISTOMORPHOMETRIC ANALYSIS AT THREE, SIX, AND 36 MONTHS (Table 1, Table 2)

Representative examples of SES and BVS 1.0 in the non-atherosclerotic rabbit iliac artery model at three, six and 36 months are shown in **Figure 2**. All implanted arteries were widely patent. At angiography, we could not evaluate fracture of BVS while no fracture was observed in the SES group. There was no difference in histologic injury score between arteries implanted with either of the two devices at all three time points. The histologic injury score varied from 0.49 to 1.23, and is considered low when assessed pathologically at the proximal, mid, and distal locations for the two devices (**Table 2**). The vessel size, as represented by IEL area, was smaller in BVS than SES implanted arteries, with this disparity between BVS and SES becoming larger over time (three months: 1.22 mm<sup>2</sup>, six months: 1.71 mm<sup>2</sup>, 36 months: 2.65 mm<sup>2</sup>), which is probably related to the histological processing, e.g., vessel shrinkage by formalin fixation and the absence of radial scaffolding force in concordance with the bioresorption of the BVS. Similarly, the lumen area was significantly smaller and % stenosis was significantly greater in BVS implanted arteries at all time points as compared to SES. Medial areas showed no remarkable change in either

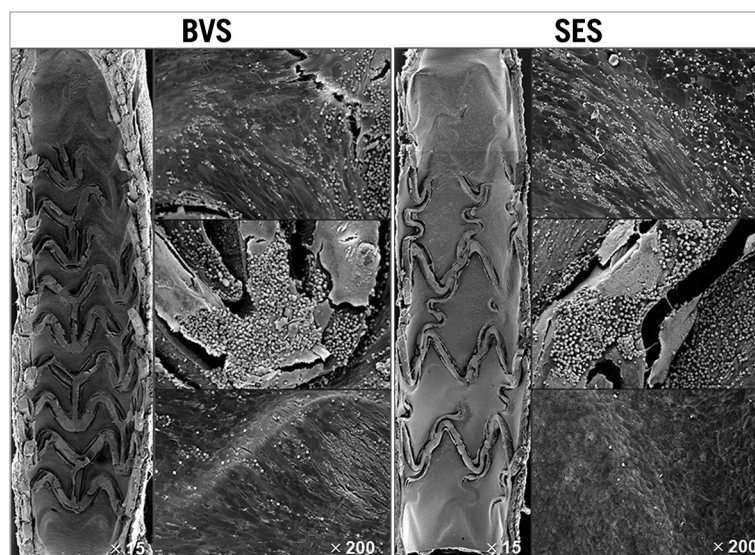


**Figure 1.** Representative SEM images at one month in BVS and SES. The proximal and distal ends of both BVS and SES were covered by a thin neointima. Exposed struts generally showed platelets and inflammatory cells. Areas between struts generally showed coverage predominated by spindle-shaped endothelial cells with poorly formed intercellular junctions.

**Table 1. Morphometric comparison of cross-sectional areas, neointimal response and injury at 3 months, 6 months and 36 months. Analysis includes mean of all implanted sections (proximal, mid, and distal).**

	3 Months (n=8)			6 Months (n=3)			36 Months (n=5)		
	SES	BVS	p-value	SES	BVS	p-value	SES	BVS	p-value
EEL area (mm <sup>2</sup> )	7.41±0.63	6.25±0.89	NS	8.02±0.52	6.31±0.25	0.007	7.51±0.7	4.85±0.94	0.0009
IEL area (mm <sup>2</sup> )	7.1±0.61	5.88±0.89	NS	7.67±0.54	5.96±0.27	0.008	7.19±0.68	4.54±0.94	0.0010
Lumen area (mm <sup>2</sup> )	6.07±0.54	4.11±0.76	<0.0001	6.66±0.51	4.35±0.20	0.002	6.07±0.58	3.49±0.79	0.0004
Neointimal area (mm <sup>2</sup> )	1.03±0.22	1.77±0.19	<0.0001	1.01±0.08	1.62±0.07	0.0006	1.11±0.2	1.06±0.19	NS
Medial area (mm <sup>2</sup> )	0.31±0.06	0.37±0.06	NS	0.35±0.05	0.35±0.02	NS	0.33±0.07	0.31±0.024	NS
% Stenosis	14.5±2.8	30.4±3.04	<0.0001	13.17±0.99	27.1±0.11	<0.0001	15.51±2.25	23.25±2.6	0.001
Mean neointimal thickness (mm)	0.06±0.03	0.17±0.03	<0.0001	0.08±0.02	0.16±0.07	0.003	0.14±0.011	0.18±0.017	0.0055

BVS 1.0 or SES at any time point (**Table 1**). Interestingly, neointimal thickness in SES implanted arteries increased over time while neointimal coverage of BVS appeared stable with no change in neointimal thickness over struts/resorption sites in BVS implanted arteries (**Figure 3**).

#### HISTOMORPHOLOGY OF BVS IN THE RABBIT ILIAC ARTERY MODEL

The results of responses reflective of vascular healing are summarised in **Table 2**. Fibrin deposition in both BVS and SES implanted arteries was mild and localised around the struts (**Table 2**). Overall,

inflammation scores for both implants were low; however, cellular inflammation, which consisted predominantly of macrophages and peri-strut giant cells, was infrequently observed in BVS 1.0 implanted arteries at six and 36 months as compared to those with SES (**Figure 4**). Re-endothelialisation was complete in BVS implanted arteries at six and 36 months, whereas SES implanted arteries showed incomplete re-endothelialisation at all time points (**Figure 3**).

Representative photomicrographs of struts (three, six months) and resorption sites (36 months) of BVS 1.0 are provided in **Figure 5** to illustrate the histomorphological changes that occur once resorption is complete. At three and six months, the polymeric struts of BVS

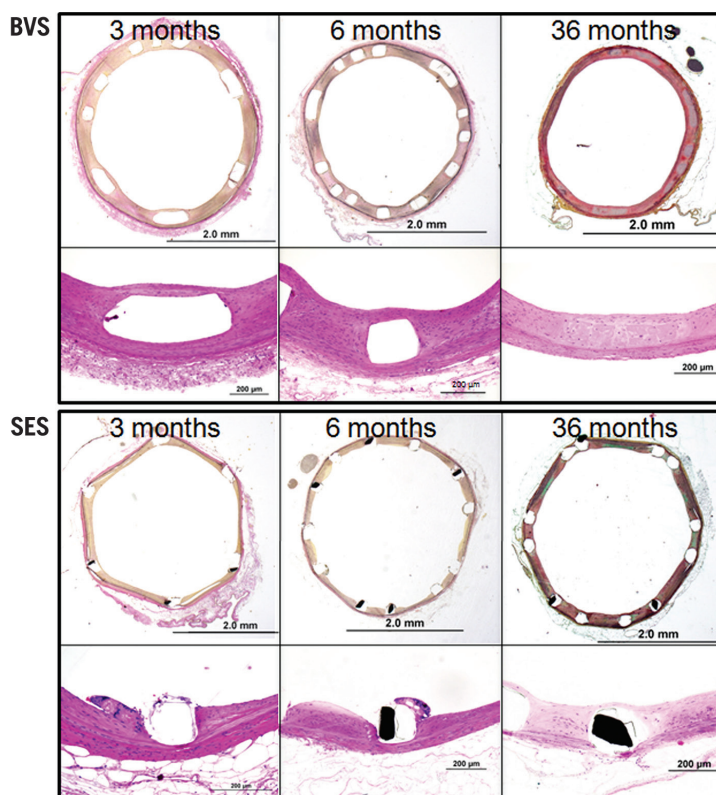


**Figure 2.** Representative photomicrographs at three, six, and 36 months of SES and BVS implanted rabbit iliac arteries. Representative low- and high-power images of SES and BVS cross-sections at three, six and 36 months. Note that resorption sites of BVS at 36 months are poorly discernible from the surrounding arterial wall. SES implanted arteries feature uncovered struts and mild inflammatory reaction at three and six months.



**Table 2. Histologic comparison of arterial healing and inflammatory response at 3 months, 6 months and 36 months. Analysis includes mean of all implanted sections.**

	3 Months (n=8)			6 Months (n=3)			36 Months (n=5)		
	SES	BVS	p-value	SES	BVS	p-value	SES	BVS	p-value
Struts with fibrin (%)	3.59±3.66	8.29±10.80	NS	15.93±15.57	1.39±2.41	NS	0.74±1.66	0.00±0.00	NS
Fibrin score	0.00±0.00	0.08±0.15	NS	0.44±0.51	0.00±0.00	NS	0.00±0.00	0.00±0.00	NS
Endothelialisation (%)	71.5±16.13	84.1±14.35	NS	88.89±10.05	100.00±0.00	NS	93.33±6.56	100.00±0.00	0.0527
Struts with giant cells (%)	41.8±13.8	37.0±9.94	NS	32.04±15.01	2.22±3.85	0.03	6.46±4.87	0.00±0.00	0.018
Intimal inflammation score	1.08±0.15	1.08±0.24	NS	1.11±0.25	0.33±0.25	NS	0.2±0.18	0.00±0.00	0.0495
Injury score	1.23±0.12	1.01±0.18	NS	0.49±0.11	0.62±0.36	NS	0.9±0.34	0.8±0.31	NS

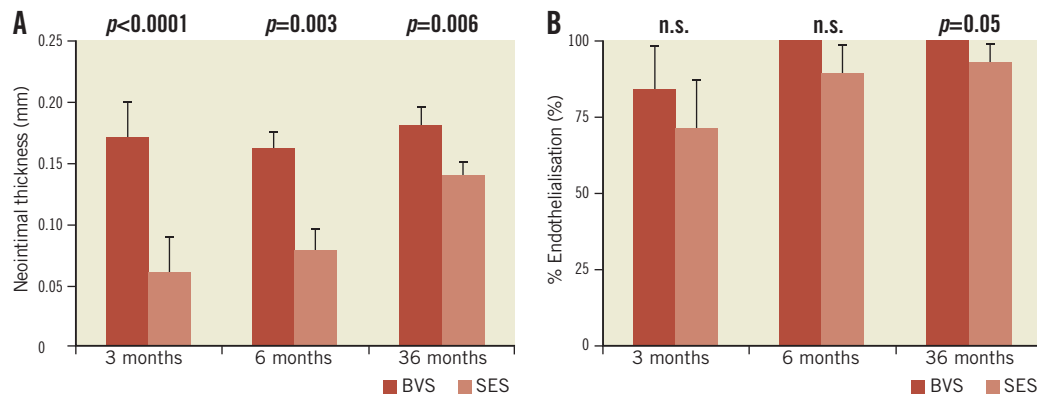


**Figure 3.** Three, six, and 36-month neointimal thickness (A) and percent endothelialisation (B) in SES and BVS implanted arteries. A) Note the late catch-up of neointimal formation in SES and no ongoing reactivity in BVS over time. B) Endothelialisation in BVS is completed at six months and still significantly greater at 36 months as compared to SES. Data are stated as mean±SD.

were well apposed to the artery wall, and by six months were sequestered from the lumen by a fibromuscular neointima with complete endothelial coverage at six months. The bioresorbable struts were readily visible at three and six months and had well-defined, squared edges, were clear and devoid of staining, and were birefringent under polarised light. At 36 months, the resorption sites (pre-existing struts) were no longer birefringent under polarised light and were poorly

discernible from the surrounding arterial wall. Resorption sites consisted of regions of amorphous material in a proteoglycan rich matrix with few scattered smooth muscle cells with or without cartilaginous metaplasia and variably surrounded and infiltrated by dense collagen. Three of the five BVS implanted arteries at 36 months showed minimal focal mineralisation, seen as linear focal streaks immediately localised around resorption sites of BVS, and cartilaginous

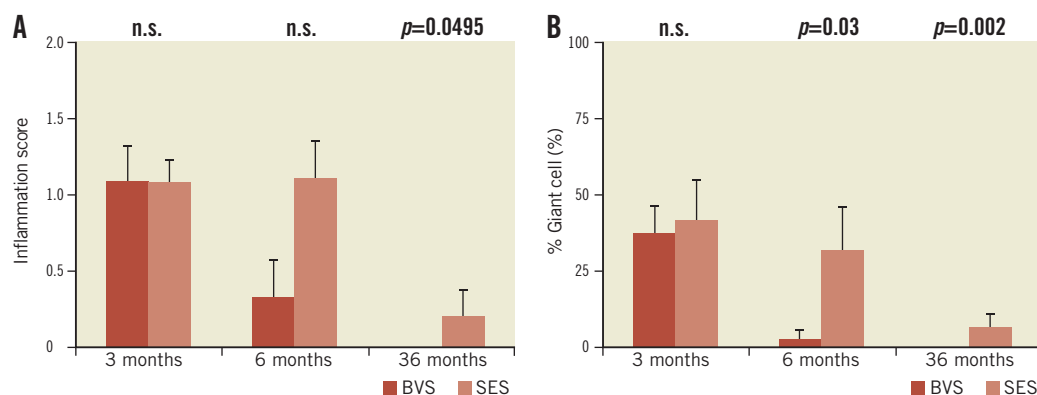


**Figure 4.** Three, six, and 36-month inflammation score (A) and giant cell formation (B) in SES and BVS. Inflammation scores trend lower in BVS implanted arteries as compared to SES implanted arteries, with an absence of inflammation at 36 months in BVS and the ongoing inflammation in SES. Data are stated as mean±SD.

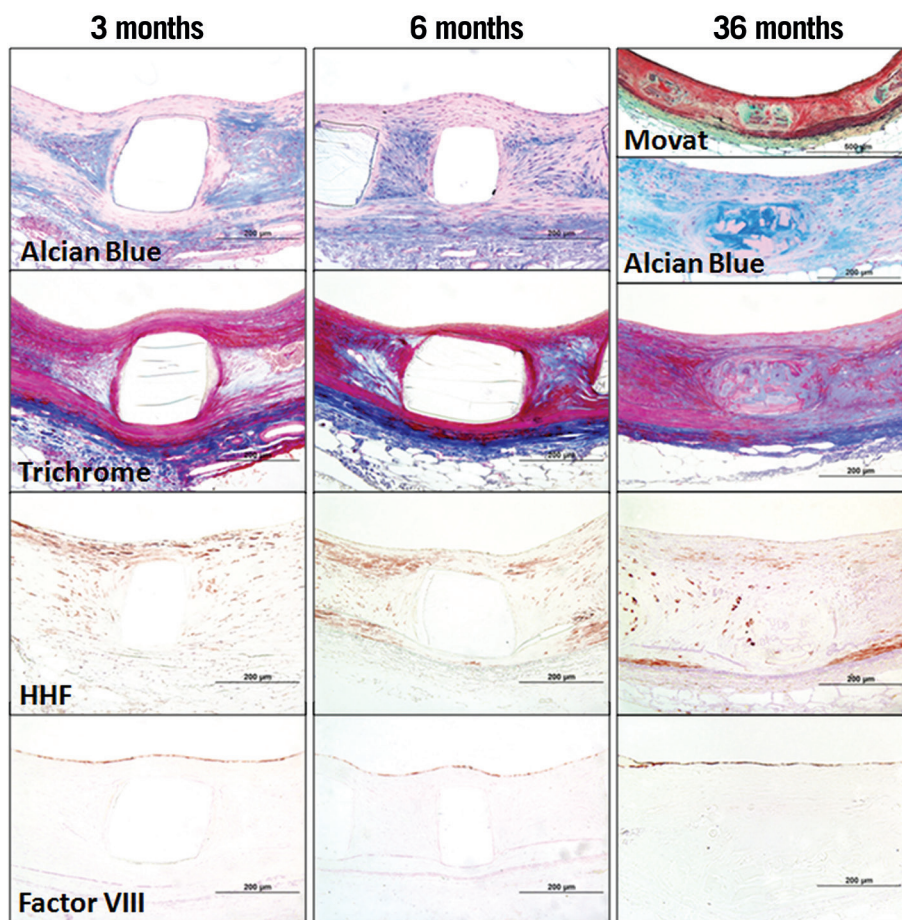


**Figure 5.** Representative photomicrographs of BVS in a rabbit iliac model at three, six, and 36 months post implantation. Representative arterial wall sections of BVS struts (three, six months) and resorption sites (36 months). The polymeric strut of BVS remains intact and unstained at three and six months. At 36 months, the resorption site of the pre-existing BVS consists of hypocellular connective tissue predominated by a proteoglycan rich matrix corresponding to the green and blue areas stained by Movat pentachrome and Alcian blue, respectively. Few smooth muscle cells (red in Masson trichrome and positive for smooth muscle actin HHF-35) are integrated into this matrix. Factor VIII staining confirms largely complete re-endothelialisation at all time points.

metaplasia, a change described in the rabbit arterial wall following biodegradable scaffold placement<sup>20</sup>. No calcification or cartilaginous metaplasia was observed in the SES group.

## Discussion

Bioresorbable vascular scaffolds present an appealing concept for balancing the requirements of preventing plaque prolapse, negative remodelling, and acute thrombosis for a short period of time following balloon dilatation and avoiding the long-term presence of foreign material that may serve as a nidus for chronic inflammation, hypersensitivity reaction, strut malapposition, and LST<sup>5</sup>. The absence of a metallic cage should allow restoration of vasomotion and improve endothelial function which may result in the prevention of neoatherosclerosis, although the mechanisms responsible for this process might be multifactorial and remain poorly understood<sup>6</sup>. Currently, several devices are under development and/or are being evaluated in preclinical and clinical trials<sup>21</sup>.

The earliest bioabsorbable device was first described by Tamai and co-workers (Igaki-Tamai stent; Igaki Medical Planning Company,

Kyoto, Japan), with implanted patients in Japan and Europe. The stent was made of poly-L-lactic acid (PLLA) in a simple coil zigzag helical design which was premounted, balloon-expandable, and also had the ability to self-expand; however, it lacked a drug coating. It showed satisfactory clinical results at six months with a 10.5% restenosis rate<sup>22</sup>. The full degradation was expected to be completed by 18 to 24 months and the cumulative rate of target lesion revascularisation was 18% at five years and 28% at 10 years<sup>23</sup>. The first generation of the Abbott Vascular BVS (BVS 1.0) was tested in 30 patients, and the two- and four-year results showed low ischaemia-driven target lesion revascularisation rates of 3.4% and 3.6%, respectively<sup>9,11</sup>.

Onuma et al published the histomorphological findings in the porcine coronary model with matching optical coherence tomography (OCT) assessment prior to sacrifice. These findings showed that BVS resorption occurs from two to three years, with substantial histomorphological changes where struts remain discernible from two years to complete resorption, and the resorption sites consist of dense, hypocellular connective tissue with hyaline areas of non-fibrillar glycoprotein<sup>7</sup>. As compared to the porcine coronary model,

the rabbit iliac arteries generally have a higher elasticity and show less inflammatory reaction. As such, the use of the rabbit iliac model allows for a reduction in these two model-dependent factors, allowing for clearer and more direct comparison of implanted devices without the potential complications of excessive injury or inflammation<sup>24,25</sup>. Results presented here in the rabbit iliac artery model show comparable morphological changes in BVS resorption sites to those observed in porcine coronary arteries, with resorption sites at three years being mostly occupied by a matrix consisting of proteoglycans and collagen, containing few cells with characteristics of smooth muscle cells, and rare sites of cartilaginous metaplasia.

In the present study, we report the results from a bioresorbable everolimus-eluting coronary scaffold with a poly-L-lactic acid polymer and a poly-D, L-lactic acid/everolimus coating in a non-atherosclerotic iliac rabbit artery showing no adverse events, complete re-endothelialisation, a smooth muscle cell dense neointimal formation at three to six months, and complete degradation and replacement of the scaffold by dense connective tissue at three years. Overall, our preclinical study deploying BVS in non-atherosclerotic rabbit iliac arteries showed mild neointimal coverage at three and six months followed by morphological changes in resorption sites occurring at 36 months. This includes vascular restoration by proteoglycan-collagenous matrix deposition and smooth muscle cell infiltration.

It has been suggested that the rabbit iliac artery model is suitable for the safety assessment of intracoronary devices since the model shows slower vascular healing and re-endothelialisation following stent implantation than the porcine model<sup>26</sup>. Incomplete re-endothelialisation has been demonstrated by SEM in the current rabbit iliac artery model in both BVS 1.1 and SES at one month, with a trend towards less coverage in the former. Delayed re-endothelialisation following BVS placement might be partly attributable to a greater area of luminal surface covered by BVS as compared to SES, but it could also be explained by thick strut thickness of BVS (156 µm) with antiproliferative drug effect. Thick struts as compared to thin struts have been shown to be associated with greater flow disturbance which probably leads to poor endothelial cell coverage<sup>27</sup>. A recent preclinical study of a porcine coronary model showed that delayed strut coverage of overlapping BVS at 28 days is almost exclusively associated with a direct overlay configuration of the BVS strut<sup>28</sup>. On the other hand, the current light microscopic assessment at a later time point showed greater endothelialisation with less inflammation in BVS as compared to SES. This might be attributable to resorption of the scaffold in BVS versus sustained inflammatory reaction to durable polymer in SES, as previous studies in a porcine coronary artery model showed an escalating amount of inflammation over time following SES placement<sup>29</sup>. Although both SES and BVS are a similar size, it may be that the polymer plays an important role during stent healing rather than just the thickness of the stent strut alone.

With respect to morphometrical results, the comparison of BVS implanted arteries to SES implanted arteries showed the former to trend towards greater neointimal thickness and percent stenosis in this preclinical model. However, BVS implanted arteries obtain a neointimal thickness that remains relatively stable in thickness

from three months to 36 months (0.17 mm), indicating stability in the vascular healing through complete degradation of the scaffold, though there was progressive compositional change in the replacement of struts to resorption sites from six to 36 months. In contrast, the neointimal thickness of SES implanted arteries gradually increases from three months to 36 months, which may be indicative of ongoing vascular healing processes, such as low-grade inflammation. This is supported by the inflammation scores obtained at six and 36 months, which were greater in SES implanted arteries as compared to BVS implanted arteries.

Regarding area measurements, it is important to take into consideration that BVS is a resorbing polymeric device and is thus subject to shrinkage which is likely to occur during formalin fixation, dehydration, and embedding in methyl methacrylate or paraffin. Decreased lumen and scaffold areas of BVS might be attributable to these artefacts or may reflect negative remodelling, especially at later time points when BVS no longer provides a scaffolding function. On the other hand, decreased lumen area in BVS was accompanied by reduced neointimal area over time; therefore, it is also possible that the bioresorption of the scaffold allows positive remodelling even though the current pathologic study failed to show enlargement of the vessel, and the smaller lumen area could be an effect of shrinkage artefacts from fixation and dehydration. Indeed, clinical studies of BVS have shown late luminal enlargement as assessed by serial OCT imaging (minimal lumen area:  $2.65 \pm 1.49 \text{ mm}^2$  at six months to  $3.80 \pm 2.42 \text{ mm}^2$  at two years)<sup>9</sup>.

Encouraging data from this and other preclinical studies evaluating BVS reflect the clinical performance obtained to date in the ABSORB trials. From the first ABSORB cohort A trial completed in July 2006, of the 29 patients, one had target lesion revascularisation at 46 days. At three years, two patients had died a non-cardiac death (one from duodenal perforation and the other from Hodgkin's lymphoma) and, of those remaining, two patients underwent non-ischaemia-driven target vessel revascularisation. Of note, no cases of stent thrombosis and a low MACE rate of 3.4% were reported at three-year follow-up<sup>10</sup>. The ABSORB cohort B trial further showed safety and efficacy of BVS (BVS 1.1) with a low rate of major adverse cardiac events (6.8%) without any scaffold thrombosis at two years<sup>14</sup>. Quantitative coronary angiography assessment showed lower late loss in BVS 1.1 (0.27 mm at two years) as compared to BVS 1.0 (0.48 mm at two years)<sup>9,14</sup>.

### Study limitations

Differences between healthy rabbit iliac arteries and diseased human arteries may limit the ability to generalise the findings of our study directly to clinical outcomes in man. In addition, animal studies have limited capability to address the process of vascular remodelling since each animal always reflects a fixed time point of follow-up and lacks underlying atherosclerosis. This study utilised two versions of bioresorbable scaffolds: BVS 1.0 and 1.1. However, there is no compositional difference (PLLA with PLLA - everolimus coating at  $100 \mu\text{g}/\text{cm}^2$ ) between the two devices. Therefore, the characteristics of the vascular response are

expected to be the same in these two devices despite the scaffold design modification, and we do not believe the modification would impact on the extent of re-endothelialisation which is governed more by the strut thickness<sup>30</sup>. The current study included a relatively small number of animals which may not allow us to identify the differences in vascular responses between BVS and SES, and therefore further studies with a larger number of animals are needed to confirm our findings.

## Conclusions

The introduction of fully bioresorbable vascular scaffolds represents an appealing concept for the interventional community for coronary and peripheral vascular applications. The current study evaluating BVS showed equivalent re-endothelialisation to SES at one month and preferential responses at later time points. This included low to no vascular inflammation, complete neointimal coverage and a comparable efficacy as compared to SES. It is likely that the fully bioresorbable everolimus-eluting scaffold with a poly-L-lactide backbone has advantages over permanent polymeric DES which have been associated with LST, and is likely to be safer in man as it is almost totally absorbed by two to three years in animal models as well as in man. However, these findings have to be confirmed in larger clinical trials and more complex lesion settings and these are currently underway.

### Impact on daily practice

The bioresorbable vascular scaffold (BVS) provides the advantage of a temporary scaffold including the antiproliferative capacity of an everolimus-eluting stent. Our preclinical study provides valuable insights into the BVS stent in a long-term rabbit iliac artery model regarding vascular healing, vessel restoration, re-endothelialisation and vascular inflammation. BVS are increasingly implanted in complex lesions, while the short and long-term outcome of these patients remains unclear. Our findings may help to understand the vascular reactions following implantation of BVS in man.

## Funding

This study is supported by a grant from Abbott Vascular, Santa Clara, CA, USA.

## Conflict of interest statement

R. Virmani receives research support from Abbott Vascular, Biosensors International, Biotronik, Boston Scientific, Medtronic, MicroPort Medical, OrbusNeich Medical, SINO Medical Technology, and Terumo Corporation; has speaking engagements with Merck; receives honoraria from Abbott Vascular, Boston Scientific, Lutonix, Medtronic, and Terumo Corporation; and is a consultant for 480 Biomedical, Abbott Vascular, Medtronic, and W.L. Gore. L. Perkins, J. Lane and R. Rapoza are employees of Abbott Vascular, Santa Clara, CA, USA. The other authors have no conflicts of interest to declare.

## References

1. Daemen J, Wenaweser P, Tsuchida K, Abrecht L, Vaina S, Morger C, Kukreja N, Jüni P, Sianos G, Hellige G, van Domburg RT, Hess OM, Boersma E, Meier B, Windecker S, Serruys PW. Early and late coronary stent thrombosis of sirolimus-eluting and paclitaxel-eluting stents in routine clinical practice: data from a large two-institutional cohort study. *Lancet*. 2007;369:667-78.
2. Joner M, Finn AV, Farb A, Mont EK, Kolodgie FD, Ladich E, Kutys R, Skorija K, Gold HK, Virmani R. Pathology of drug-eluting stents in humans: delayed healing and late thrombotic risk. *J Am Coll Cardiol*. 2006;48:193-202.
3. Finn AV, Kolodgie FD, Harnek J, Guerrero LJ, Acampado E, Tefera K, Skorija K, Weber DK, Gold HK, Virmani R. Differential response of delayed healing and persistent inflammation at sites of overlapping sirolimus- or paclitaxel-eluting stents. *Circulation*. 2005;112:270-8.
4. Virmani R, Guagliumi G, Farb A, Musumeci G, Grieco N, Motta T, Mihalcsik L, Tsepili M, Valsecchi O, Kolodgie FD. Localized hypersensitivity and late coronary thrombosis secondary to a sirolimus-eluting stent: should we be cautious? *Circulation*. 2004;109:701-5.
5. Nakazawa G, Finn AV, Vorpahl M, Ladich ER, Kolodgie FD, Virmani R. Coronary responses and differential mechanisms of late stent thrombosis attributed to first-generation sirolimus- and paclitaxel-eluting stents. *J Am Coll Cardiol*. 2011;57:390-8.
6. Nakazawa G, Otsuka F, Nakano M, Vorpahl M, Yazdani SK, Ladich E, Kolodgie FD, Finn AV, Virmani R. The pathology of neo-atherosclerosis in human coronary implants: bare-metal and drug-eluting stents. *J Am Coll Cardiol*. 2011;57:1314-22.
7. Onuma Y, Serruys PW, Perkins LE, Okamura T, Gonzalo N, Garcia-Garcia HM, Regar E, Kamberi M, Powers JC, Rapoza R, van Beusekom H, van der Giessen W, Virmani R. Intracoronary optical coherence tomography and histology at 1 month and 2, 3, and 4 years after implantation of everolimus-eluting bioresorbable vascular scaffolds in a porcine coronary artery model: an attempt to decipher the human optical coherence tomography images in the ABSORB trial. *Circulation*. 2010;122:2288-300.
8. Ormiston JA, Serruys PW, Regar E, Dudek D, Thuesen L, Webster MW, Onuma Y, Garcia-Garcia HM, McGreevy R, Veldhof S. A bioabsorbable everolimus-eluting coronary stent system for patients with single de-novo coronary artery lesions (ABSORB): a prospective open-label trial. *Lancet*. 2008;371:899-907.
9. Serruys PW, Ormiston JA, Onuma Y, Regar E, Gonzalo N, Garcia-Garcia HM, Nieman K, Bruining N, Dorange C, Miquel-Hebert K, Veldhof S, Webster M, Thuesen L, Dudek D. A bioabsorbable everolimus-eluting coronary stent system (ABSORB): 2-year outcomes and results from multiple imaging methods. *Lancet*. 2009;373:897-910.
10. Onuma Y, Serruys PW, Ormiston JA, Regar E, Webster M, Thuesen L, Dudek D, Veldhof S, Rapoza R. Three-year results of clinical follow-up after a bioresorbable everolimus-eluting scaffold in patients with de novo coronary artery disease: the ABSORB trial. *EuroIntervention*. 2010;6:447-53.



11. Dudek D, Onuma Y, Ormiston JA, Thuesen L, Miquel-Hebert K, Serruys PW. Four-year clinical follow-up of the ABSORB everolimus-eluting bioresorbable vascular scaffold in patients with de novo coronary artery disease: the ABSORB trial. *EuroIntervention*. 2012;7:1060-1.
12. Serruys PW, Onuma Y, Ormiston JA, de Bruyne B, Regar E, Dudek D, Thuesen L, Smits PC, Chevalier B, McClean D, Koolen J, Windecker S, Whitbourn R, Meredith I, Dorange C, Veldhof S, Miquel-Hebert K, Rapoza R, Garcia-Garcia HM. Evaluation of the second generation of a bioresorbable everolimus drug-eluting vascular scaffold for treatment of de novo coronary artery stenosis: six-month clinical and imaging outcomes. *Circulation*. 2010;122:2301-12.
13. Serruys PW, Onuma Y, Dudek D, Smits PC, Koolen J, Chevalier B, de Bruyne B, Thuesen L, McClean D, van Geuns RJ, Windecker S, Whitbourn R, Meredith I, Dorange C, Veldhof S, Hebert KM, Sudhir K, Garcia-Garcia HM, Ormiston JA. Evaluation of the second generation of a bioresorbable everolimus-eluting vascular scaffold for the treatment of de novo coronary artery stenosis: 12-month clinical and imaging outcomes. *J Am Coll Cardiol*. 2011;58:1578-88.
14. Ormiston JA, Serruys PW, Onuma Y, van Geuns RJ, de Bruyne B, Dudek D, Thuesen L, Smits PC, Chevalier B, McClean D, Koolen J, Windecker S, Whitbourn R, Meredith I, Dorange C, Veldhof S, Hebert KM, Rapoza R, Garcia-Garcia HM. First serial assessment at 6 months and 2 years of the second generation of absorb everolimus-eluting bioresorbable vascular scaffold: a multi-imaging modality study. *Circ Cardiovasc Interv*. 2012;5:620-32.
15. Farb A, Tang AL, Shroff S, Sweet W, Virmani R. Neointimal responses 3 months after (32)P beta-emitting stent placement. *Int J Radiat Oncol Biol Phys*. 2000;48:889-98.
16. Joner M, Nakazawa G, Finn AV, Quee SC, Coleman L, Acampado E, Wilson PS, Skoriya K, Cheng Q, Xu X, Gold HK, Kolodgie FD, Virmani R. Endothelial cell recovery between comparator polymer-based drug-eluting stents. *J Am Coll Cardiol*. 2008;52:333-42.
17. Schwartz RS, Huber KC, Murphy JG, Edwards WD, Camrud AR, Vlietstra RE, Holmes DR. Restenosis and the proportional neointimal response to coronary artery injury: results in a porcine model. *J Am Coll Cardiol*. 1992;19:267-74.
18. Carter AJ, Aggarwal M, Kopia GA, Tio F, Tsao PS, Kolata R, Yeung AC, Llanos G, Dooley J, Falotico R. Long-term effects of polymer-based, slow-release, sirolimus-eluting stents in a porcine coronary model. *Cardiovasc Res*. 2004;63:617-24.
19. Finn AV, Joner M, Nakazawa G, Kolodgie F, Newell J, John MC, Gold HK, Virmani R. Pathological correlates of late drug-eluting stent thrombosis: strut coverage as a marker of endothelialization. *Circulation*. 2007;115:2435-41.
20. Hietala EM, Salminen US, Stahls A, Valimaa T, Maasilta P, Tormala P, Nieminen MS, Harjula AL. Biodegradation of the copolymeric polylactide stent. Long-term follow-up in a rabbit aorta model. *J Vasc Res*. 2001;38:361-9.
21. Onuma Y, Ormiston J, Serruys PW. Bioresorbable scaffold technologies. *Circ J*. 2011;75:509-20.
22. Tamai H, Igaki K, Kyo E, Kosuga K, Kawashima A, Matsui S, Komori H, Tsuji T, Motohara S, Uehata H. Initial and 6-month results of biodegradable poly-l-lactic acid coronary stents in humans. *Circulation*. 2000;102:399-404.
23. Nishio S, Kosuga K, Igaki K, Okada M, Kyo E, Tsuji T, Takeuchi E, Inuzuka Y, Takeda S, Hata T, Takeuchi Y, Kawada Y, Harita T, Seki J, Akamatsu S, Hasegawa S, Bruining N, Brugaletta S, de Winter S, Muramatsu T, Onuma Y, Serruys PW, Ikeguchi S. Long-Term (>10 Years) clinical outcomes of first-in-human biodegradable poly-l-lactic acid coronary stents: Igaki-Tamai stents. *Circulation*. 2012;125:2343-53.
24. Kornowski R, Hong MK, Tio FO, Bramwell O, Wu H, Leon MB. In-stent restenosis: contributions of inflammatory responses and arterial injury to neointimal hyperplasia. *J Am Coll Cardiol*. 1998;31:224-30.
25. Wilson GJ. Interpreting arterial wall inflammation around stents in the porcine coronary artery model. *J Vasc Interv Radiol*. 2011;22:260-1.
26. Finn AV, Nakazawa G, Joner M, Kolodgie FD, Mont EK, Gold HK, Virmani R. Vascular responses to drug eluting stents: importance of delayed healing. *Arterioscler Thromb Vasc Biol*. 2007;27:1500-10.
27. Kolandaivelu K, Swaminathan R, Gibson WJ, Kolachalama VB, Nguyen-Ehrenreich KL, Giddings VL, Coleman L, Wong GK, Edelman ER. Stent thrombogenicity early in high-risk interventional settings is driven by stent design and deployment and protected by polymer-drug coatings. *Circulation*. 2011;123:1400-9.
28. Farooq V, Serruys PW, Heo JH, Gogas BD, Onuma Y, Perkins LE, Diletti R, Radu MD, Raber L, Bourantas CV, Zhang Y, van Remortel E, Pawar R, Rapoza RJ, Powers JC, van Beusekom HM, Garcia-Garcia HM, Virmani R. Intracoronary optical coherence tomography and histology of overlapping everolimus-eluting bioresorbable vascular scaffolds in a porcine coronary artery model: the potential implications for clinical practice. *JACC Cardiovasc Interv*. 2013;6:523-32.
29. Nakazawa G, Finn AV, Ladich E, Ribichini F, Coleman L, Kolodgie FD, Virmani R. Drug-eluting stent safety: findings from preclinical studies. *Expert Rev Cardiovasc Ther*. 2008;6:1379-91.
30. Simon C, Palmaz JC, Sprague EA. Influence of topography on endothelialization of stents: clues for new designs. *J Long Term Eff Med Implants*. 2000;10:143-51.